

1 2 3 4 1 **Transcriptional mapping of the primary somatosensory cortex upon sensory deprivation**

5
6 2 Koen Kole^{1,2}, Yutaro Komuro¹, Jan Provaznik³, Jelena Pistolic³,

7
8 3 Vladimir Benes³, Paul Tiesinga², Tansu Celikel¹

9
10 4 (1) Department of Neurophysiology, (2) Department of Neuroinformatics, Donders Institute for
11 5 Brain, Cognition, and Behaviour, Radboud University, Nijmegen - the Netherlands. (3) European
12 6 Molecular Biology Laboratory (EMBL), Genomics Core Facility, Heidelberg - Germany

13
14 7 E-mail addresses (in the order of appearance): k.kole@neurophysiology.nl,
15 8 y.komuro@neurophysiology.nl, jan.provaznik@embl.de, jelena.pistollic@embl.de,
16 9 benes@embl.de, p.tiesinga@science.ru.nl, celikel@neurophysiology.nl (corresponding author)

18 19 10 20 11 **Background (162)**

21
22 12 Experience-dependent plasticity (EDP) is essential for anatomical and functional maturation of
23 13 sensory circuits during development. Although the principal synaptic and circuit mechanisms of
24 14 EDP are experimentally and computationally increasingly well studied, its molecular mechanisms
25 15 remain largely elusive. EDP can be readily studied in the rodent barrel cortex. Each 'barrel column'
26 16 topographically is linked to the principal whisker that forms its main source of input. Depriving
27 17 select whiskers while sparing their neighbours introduces competition between barrel columns,
28 18 ultimately leading to weakening of intracortical, translaminal (i.e. Cortical Layer (L)4-to-L2/3) feed-
29 19 forward excitatory projections in the deprived columns. The same synapses are potentiated in the
30 20 neighbouring spared columns. These experience-dependent, and cortical column- and layer-
31 21 specific, alterations of synaptic strength are thought to underlie somatosensory map plasticity.
32 22 We used RNA sequencing in this model system to uncover cortical-column and -layer specific
33 23 changes on the transcriptome level that are induced by altered sensory experience. This resource
34 24 will help to systematically address the molecular processes that underlie cortical plasticity.

35 36 37 38 25 **Findings (47)**

39
40 26 From column- and layer-specific barrel cortical tissue, high quality RNA was purified and
41 27 sequenced. The current dataset entails an average of 50 million paired-end reads per sample, 75
42 28 base pairs in length. On average, 90.15% of reads could be uniquely mapped to the mm10
43 29 reference mouse genome.

44 45 46 30 **Conclusions (32) – Word total for the abstract: 241 out of 250**

47
48 31 The current data reveal the transcriptional changes in gene expression in the barrel cortex upon
49 32 altered sensory experience in juvenile animals and will help to molecularly map the mechanisms
50 33 of cortical plasticity.

51
52
53
54
55
56
57
58
59
60
61
62
63
64
65

1
2
3
4
5
6
7
8
9
10
11
12
13
14
15
16
17
18
19
20
21
22
23
24
25
26
27
28
29
30
31
32
33
34
35
36
37
38
39
40
41
42
43
44
45
46
47
48
49
50
51
52
53
54
55
56
57
58
59
60
61
62
63
64
65

34 **Data Description**

35 Sensory experience powerfully shapes neural circuits. Changes due to sensory organ deprivation
36 such as eye closure, digit amputation, and whisker trimming provide powerful means for studying
37 mechanisms of experience dependent cortical plasticity.

38 In the whisker system experience dependent plasticity is most commonly studied in the
39 barrel cortex subfield of the primary somatosensory cortex where neural representations of
40 whiskers change in response to altered patterns of incoming sensory information. As originally
41 shown in the barrel cortex (Hand 1982), sensory deprivation induced by transient whisker
42 trimming is sufficient to perturb neural receptive fields both during development and in adulthood.
43 Previous work has also shown that the cellular basis of deprivation-induced decreases in whisker
44 evoked representations are primarily due to a reduction of synaptic strength in monosynaptically
45 connected feed-forward neuronal networks in behaving animals (Allen et al. 2003; Celikel et al.
46 2004). Conversely whisker sparing induced enhancement in whisker representation is mediated
47 at least in part by the long-term synaptic facilitation expressed along the L4 projections *in vivo*
48 (Clem et al. 2008). Identification of the molecular events that mediate these bidirectional changes
49 in synaptic connectivity will benefit from systematic analysis of the gene transcription. Therefore,
50 we performed RNA sequencing in the barrel cortex with or without sensory deprivation across
51 cortical layers 2-4. This database will assist molecular and cellular neurobiologists in addressing
52 the molecular mechanisms associated with experience dependent plasticity, and will enable
53 statistical approaches to determine the dynamics of the coupled changes across molecular
54 pathways as cortical circuits undergo plastic changes in their organization.

56 **Animals**

57 All experiments were performed in accordance with the Animal Ethics Committee of the Radboud
58 University in Nijmegen, the Netherlands. Pregnant wild type mice (Charles River) were kept at a
59 12-hour light/dark cycle with access to food *ad libitum*. Cages were checked for birth daily. To

1
2
3
4 60 induce experience-dependent plasticity, pups underwent bilateral plucking of their C-row whiskers
5
6 61 under isoflurane anaesthesia at P12 (**Figure 1**). Control animals were not plucked but
7
8 62 anaesthetized and handled similarly. After recovery pups were returned to their home cage. Every
9
10 63 other day pups were checked for whisker regrowth, which were plucked if present. At P23-P24,
11
12 64 pups were randomly selected from their litter for slice preparation and tissue collection. For each
13
14 65 experimental condition (i.e. whisker deprived or control), 4 female pups were used.
15
16
17
18
19

20 67 *Figure 1 is about here*
21

22 68 23 24 69 **Slice preparation and sample collection**

25
26 70 Pups were anaesthetized using isoflurane and then perfused with ice cold carbogenated slicing
27
28 71 medium (108 mM ChCl, 3 mM KCl, 26 mM NaHCO₃, 1.25 mM NaH₂PO₄, 25 mM glucose, 1 mM
29
30 72 CaCl₂, 6 mM MgSO₄ and 3 mM Na-pyruvate). Next, pups were decapitated, after which the brain
31
32 73 was quickly dissected out and 400 µm thalamocortical slices from each hemisphere were
33
34 74 prepared as described before (Allen et al. 2003; Celikel et al. 2004). Slices were transferred to 37
35
36 75 degrees Celcius carbogenated ACSF (120 mM NaCl, 3.5 mM KCl, 10 mM glucose, 2.5 mM CaCl₂,
37
38 76 1.3 mM MgSO₄, 25 mM NaHCO₃ and 1.25 mM NaH₂PO₄) where they were kept for 30 minutes
39
40 77 and recovered at room temperature for another 30 minutes until tissue collection.
41
42
43

44 78
45
46 79 After incubation, slices were placed under a Nikon Eclipse FN1 microscope. The holding chamber
47
48 80 was continuously perfused with room temperature carbogenated ACSF. Due to the 55 degree
49
50 81 cut, slices were obtained in which S1 barrels from specific rows (A-E) could be identified. A thin,
51
52 82 long glass pipette was pulled using a Sutter instruments P-2000 pipette puller and was used to
53
54 83 make intercolumnar incisions from L1 to the bottom of L4 after which the slice was placed under
55
56 84 a binocular dissection microscope where the location of specific barrel columns could now be
57
58 85 readily identified by eye. A sterile 32G needle was then used to cut out L2/3 and L4 separately
59
60
61
62
63
64
65

1
2
3
4
5
6
7
8
9
10
11
12
13
14
15
16
17
18
19
20
21
22
23
24
25
26
27
28
29
30
31
32
33
34
35
36
37
38
39
40
41
42
43
44
45
46
47
48
49
50
51
52
53
54
55
56
57
58
59
60
61
62
63
64
65

86 from each column. Tissue from columns A/E and B/D were pooled as they both constitute second
87 and first order spared whiskers, respectively. Immediately after dissection, tissue samples were
88 snap frozen in liquid nitrogen and stored at -80 degrees Celcius until further use. All tools that
89 came into direct contact with brain tissue were treated using RNaseZap in order to minimize
90 RNase contamination.

91

92 RNA isolation and quality control

93 Tissue samples originating from the same rows and layers were pooled within each animal.
94 Tissue was quickly dissolved in Qiazol (Qiagen #79306), after which RNA was isolated using the
95 miRNeasy Mini kit (Qiagen #217004), DNase treated (Thermo Scientific, #EN0521) and cleaned
96 up using RNeasy MinElute kit (Qiagen #74204), all following the manufacturer's instructions.
97 Samples were then stored at -80 degrees Celcius until further processing.

98

99 RNA sample integrity was determined using Agilent Tapestation (High Sensitivity RNA
100 Screentape). Sample RINs ranged from 7.1 to 8.8. To further assess RNA purity and integrity,
101 RNA samples were used in RT-PCR to confirm that cDNA could be produced and that a large
102 (~1000 bp) amplicon could be obtained. To produce cDNA, SuperScript® II Reverse
103 Transcriptase (Thermo Scientific #18064014) and random hexamer primers (Roche
104 #11034731001) were used. The resulting cDNA was then added to a PCR reaction mix which
105 further consisted of Jumpstart Ready Mix (Sigma P2893) and exon-exon junction spanning
106 CamKII primers (FW TCCAACATTGTACGCCTCCAT; RV TGTTGGTGCTGTCGGAAGAT).
107 From all cDNA samples a fragment of the expected size could be amplified, suggesting that the
108 RNA samples contained pure RNA of sufficient integrity. All RNA samples thus passed our quality
109 control criteria and were subjected to RNA sequencing.

110

111

1
2
3
4 **112 RNA sequencing**

5
6 **113** RNA sequencing was conducted at the Genomics Core Facility of the EMBL, Heidelberg,
7
8
9 **114** Germany. The cDNA library was generated using the non-stranded NEBNext Ultra RNA Library
10
11 **115** Preparation Kit for Illumina (New England Biolabs, catalogue #E7530), which includes oligo-dT
12
13 **116** bead selection of mRNA. For library enrichment, 13-14 PCR cycles were performed. Pooled
14
15 **117** libraries were sequenced on the Illumina NextSeq 500 instrument in a 75bp paired-end mode
16
17
18 **118** using High output flow cells.

19
20 **119**
21
22 **120** Sequencing read quality was assessed using FastQC (Babraham Bioinformatics), the results of
23
24 **121** which were merged using MultiQC (<http://multiqc.info>). Results are displayed in **Figure 2**. Per
25
26 **122** base quality *phred* scores range from 34.80 to 35.15, indicating base call accuracies of >99.9%
27
28
29 **123** (**Figure 2A**). Overall 91.48-94.03% of reads had a mean *phred* score of 30 or above (**Figure 2B**).
30
31 **124** In line with these scores, per base N content (i.e. percentage of bases that could not confidently
32
33 **125** called) was very low, with a maximum value 0.053%.

34
35 **126**
36
37
38 **127** *Figure 2 is about here*
39

40 **128**
41
42 **129** Reads were then mapped to the mm10 reference genome using STAR (Dobin et al. 2013), which
43
44 **130** uniquely mapped between 39,000,000 and 59,000,000 reads, constituting an average 90.15%
45
46 **131** unique map rate across samples (**Figure 2D**). Since the library preparation protocol entails a PCR
47
48
49 **132** enrichment step which can lead to technical duplication, hence an overestimation of observed
50
51 **133** transcripts, we used Seqmonk (Babraham Bioinformatics) to plot the read density against the
52
53 **134** duplication levels (i.e. the percentage of duplicate reads) for each transcript. The obtained
54
55 **135** duplication plots showed a clear positive relation between read density and duplication levels
56
57
58 **136** (**Figure 3** and **Supplemental Figure 1**), suggesting that the origin of read duplication is biological,
59
60 **137** rather than technical.
61
62
63
64
65

1
2
3
4
5
6
7
8
9
10
11
12
13
14
15
16
17
18
19
20
21
22
23
24
25
26
27
28
29
30
31
32
33
34
35
36
37
38
39
40
41
42
43
44
45
46
47
48
49
50
51
52
53
54
55
56
57
58
59
60
61
62
63
64
65

138 Based on the above quality control measures we determined that our RNA-sequencing data was
139 of sufficient quality to be used in downstream analyses, therefore we continued with gene
140 expression analysis.

Figure 3 is about here

Analysis of gene expression

146 Using a 2 read cut-off, we identified 16,900 to 17,600 transcripts per sample (**Figure 4A**). Raw
147 gene counts can be found online (see Supporting Data – DOI to appear). Differential gene
148 expression analyses across groups were performed using EdgeR v3.12.1 (Robinson et al. 2010;
149 McCarthy et al. 2012) using only genes with a count per million (CPM) >1 in all of the samples
150 within each group (**Supplementary Table 1** for details on the commands used). Since laminar
151 identity is an important feature of our experimental setup, we assessed the relative expression of
152 known molecular markers for L2/3 (*Cacna1h, Id2, Igfbp4, Igfn1, Mdga1, Plcxd1, Rasgrf2, Rgs8,*
153 *Tle3*) and L4 (*Cartpt, Cyp39a1, Kcnh5, Kcnip2, Lmo3, Rorb, Scnn1a*) (Rowell et al. 2010; Xue et
154 al. 2014; Molyneaux et al. 2015), which showed selective enrichment of the laminar markers in
155 isolated layers (**Figure 4B**).

Figure 4 is about here

159 To assess the variance in transcript counts between experimental groups, we calculated the
160 coefficient of variation (CV) of each group with a cut-off of 50 as the minimal read count (**Figure**
161 **4C**). This analysis showed that 85.93% of transcripts have a CV below 15%, suggesting the
162 overall variance in our dataset is low.

1
2
3
4
5
6
7
8
9
10
11
12
13
14
15
16
17
18
19
20
21
22
23
24
25
26
27
28
29
30
31
32
33
34
35
36
37
38
39
40
41
42
43
44
45
46
47
48
49
50
51
52
53
54
55
56
57
58
59
60
61
62
63
64
65

164 These quality control routines suggest that we have obtained RNA-sequencing data of high read
165 quality, with individual bases being called confidently throughout the length of reads, which
166 uniquely map to the mm10 reference genome at high rates (>90% average). The laminar origin
167 of our samples could be identified through known molecular markers, confirming our samples are
168 of high anatomical specificity. This RNA-seq dataset should prove useful for researchers
169 interested in the molecular underpinnings of cortical experience-dependent plasticity.

170

171 **References**

172

173 **Allen CB, Celikel T, Feldman DE.** Long-term depression induced by sensory deprivation during
174 cortical map plasticity in vivo. *Nat Neurosci* 6: 291–9, 2003.

175 **Celikel T, Szostak VA, Feldman DE.** Modulation of spike timing by sensory deprivation during
176 induction of cortical map plasticity. *Nat Neurosci* 7: 534–41, 2004.

177 **Clem RL, Celikel T, Barth AL.** Ongoing in vivo experience triggers synaptic metaplasticity in the
178 neocortex. *Science* 319: 101–4, 2008.

179 **Dobin A, Davis CA, Schlesinger F, Drenkow J, Zaleski C, Jha S, Batut P, Chaisson M,
180 Gingeras TR.** STAR: ultrafast universal RNA-seq aligner. *Bioinformatics* 29: 15, 2013.

181 **Hand PJ** Plasticity of the rat cortical barrel system. In: Strick P, Morrison AD (eds) *Changing
182 concepts of the nervous system.* Academic Press, New York, pp 49–75, 1982

183 **McCarthy DJ, Chen Y, Smyth GK.** Differential expression analysis of multifactor RNA-Seq
184 experiments with respect to biological variation. *Nucleic Acids Res* 40: 4288, 2012.

185 **Molyneaux BJ, Goff LA, Rinn JL, Arlotta P.** Genome-wide Analysis of In Vivo Transcriptional
186 Dynamics during Pyramidal Neuron Fate Selection in Neocortex NeuroResource DeCoN:
187 Genome-wide Analysis of In Vivo Transcriptional Dynamics during Pyramidal Neuron Fate
188 Selection in Neocortex. .

189 **Robinson MD, McCarthy DJ, Smyth GK.** edgeR: a Bioconductor package for differential
190 expression analysis of digital gene expression data. *Bioinformatics* 26: 139, 2010.

191 **Rowell JJ, Mallik AK, Dugas-Ford J, Ragsdale CW.** Molecular analysis of neocortical layer
192 structure in the ferret. *J Comp Neurol* 518: 3272–3289, 2010.

193 **Xue M, Atallah B V., Scanziani M.** Equalizing excitation–inhibition ratios across visual cortical
194 neurons. *Nature* 511: 596–600, 2014.

195

1
2
3
4
5
6
7
8
9
10
11
12
13
14
15
16
17
18
19
20
21
22
23
24
25
26
27
28
29
30
31
32
33
34
35
36
37
38
39
40
41
42
43
44
45
46
47
48
49
50
51
52
53
54
55
56
57
58
59
60
61
62
63
64
65

Availability of the supporting data

Supporting data are available online (<https://goo.gl/tBof51>) and will be distributed via GigaScience DB.

Raw sequence reads were deposited in NCBI GEO.

Link: <https://www.ncbi.nlm.nih.gov/geo/query/acc.cgi?acc=GSE90929>

List of abbreviations

EDP Experience dependent plasticity

L2/3 Cortical Layer 2/3, also known as supragranular layers

L4 Cortical Layer 4, i.e. granular layer

Competing interests

The authors declare no competing interests.

Author contributions

KK performed all experimental manipulations, sample acquisition, biological and bioinformatic quality controls, and prepared the tables and figures. YK and JaP performed bioinformatic analysis. JeP performed library prep. VB supervised RNA-seq. PT contributed bioinformatic analysis and co-supervised the project. TC designed and supervised the project. KK and TC wrote the manuscript. All authors edited otherwise approved the final version of the manuscript.

1
2
3
4
5
6
7
8
9
10
11
12
13
14
15
16
17
18
19
20
21
22
23
24
25
26
27
28
29
30
31
32
33
34
35
36
37
38
39
40
41
42
43
44
45
46
47
48
49
50
51
52
53
54
55
56
57
58
59
60
61
62
63
64
65

Figure Legends

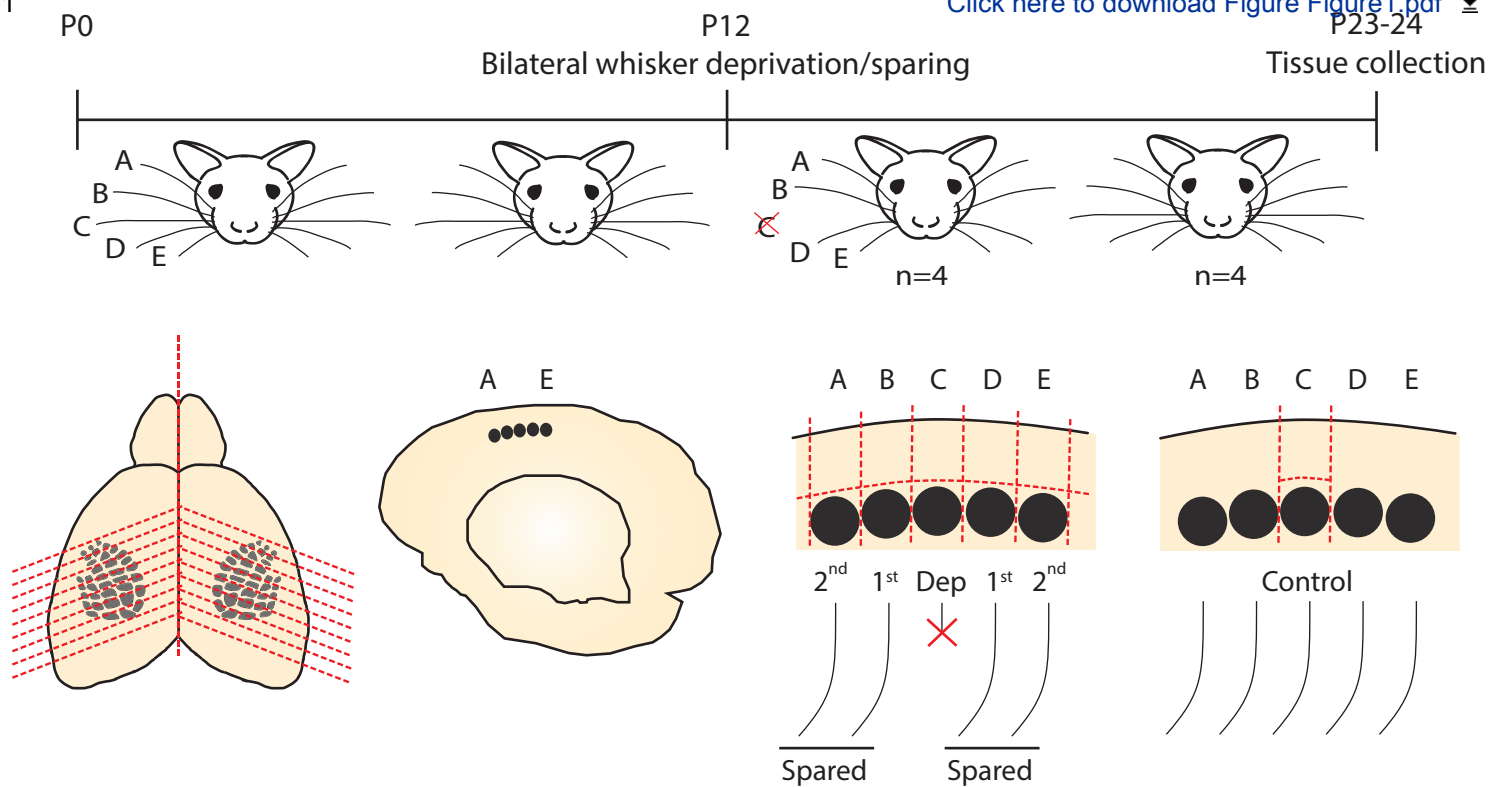
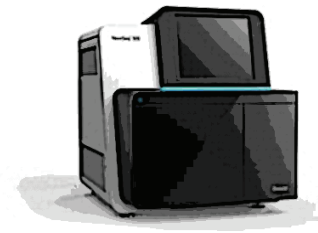
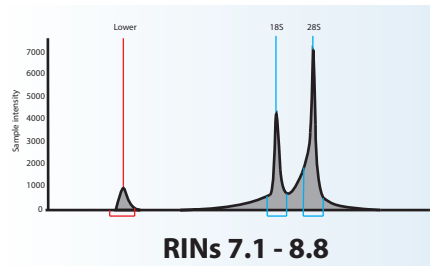
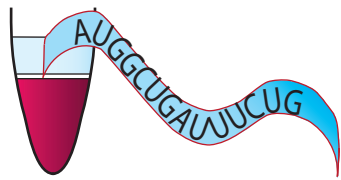
Figure 1. Overview of the experimental design, sample collection and data organization. **(A)** Pups were bilaterally spared or deprived of off their C-row whiskers between P12 and P23-P24, when acute slices are made and column- and layer-specific tissues were excised. **(B)** RNA was isolated, checked for integrity and purity, and subsequently sequenced. **(C)** Organization of the database. Colour codes denote experimental groups. Same denominations are used in the read counts matrix file (see **Supplemental Data**).

Figure 2. FastQC and STAR output graphs for all samples. **(A-B)** *Phred* scores per base and per sequence. **(C)** Per sequence GC content. **(D)** STAR output of alignment scores.

Figure 3. Overlays of duplication plot contours, showing a positive correlation between read density and duplication levels. Depicted contours enclose 90% of the data points.

Figure 4. Gene expression analyses. **(A)** Histogram of read counts per transcript per sample. With a cut-off of 2 reads, between 16,900 and 17,600 transcripts could be identified across samples. **(B)** Relative expression of known molecular markers for cortical laminae. Layer 4 markers are enriched in samples originating from this layer; the same is true for Layer 2/3 marker expression in Layer 2/3 samples. **(C)** Cumulative plot of the coefficient of variance (CV) averaged across groups. CVs of <15% are found in ~85% of transcripts.

Supplemental Figure 1. Duplication plots for all samples, produced using SeqMonk (Babraham Bioinformatics).

**B**

RNA isolation, quality control and sequencing

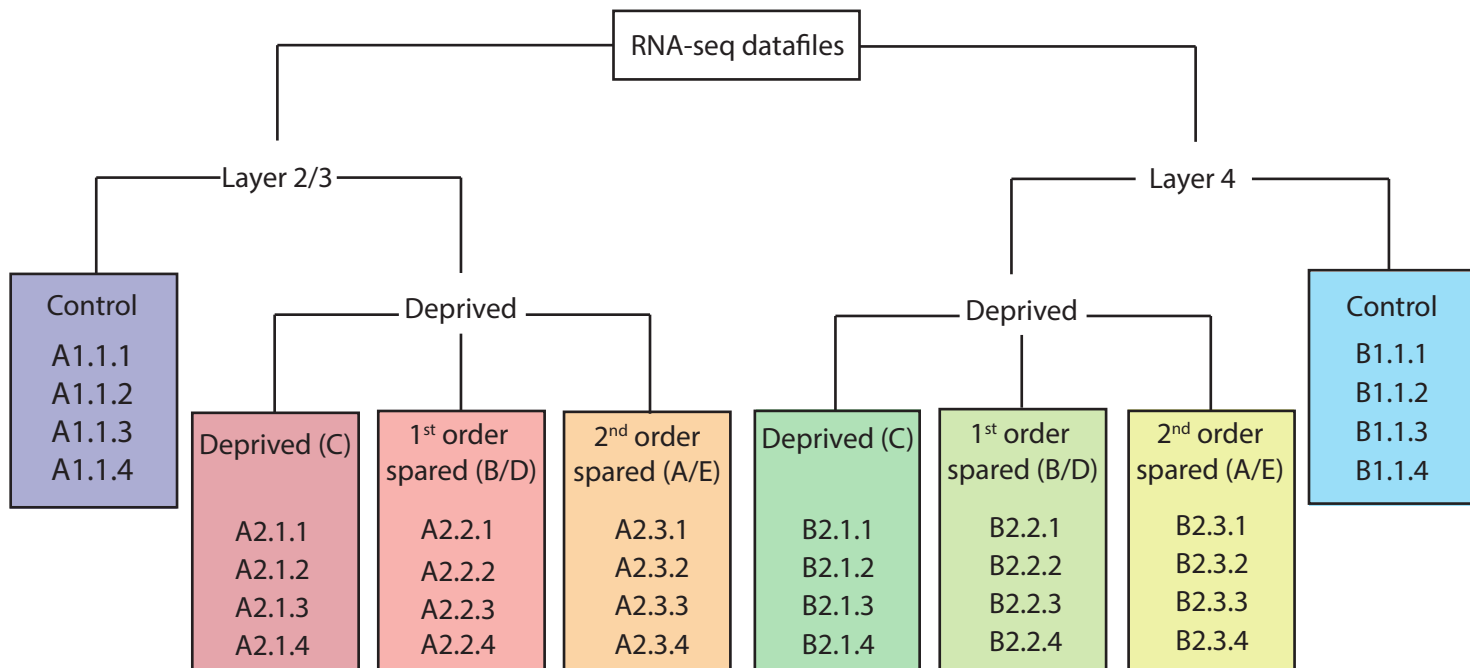
C

Figure2

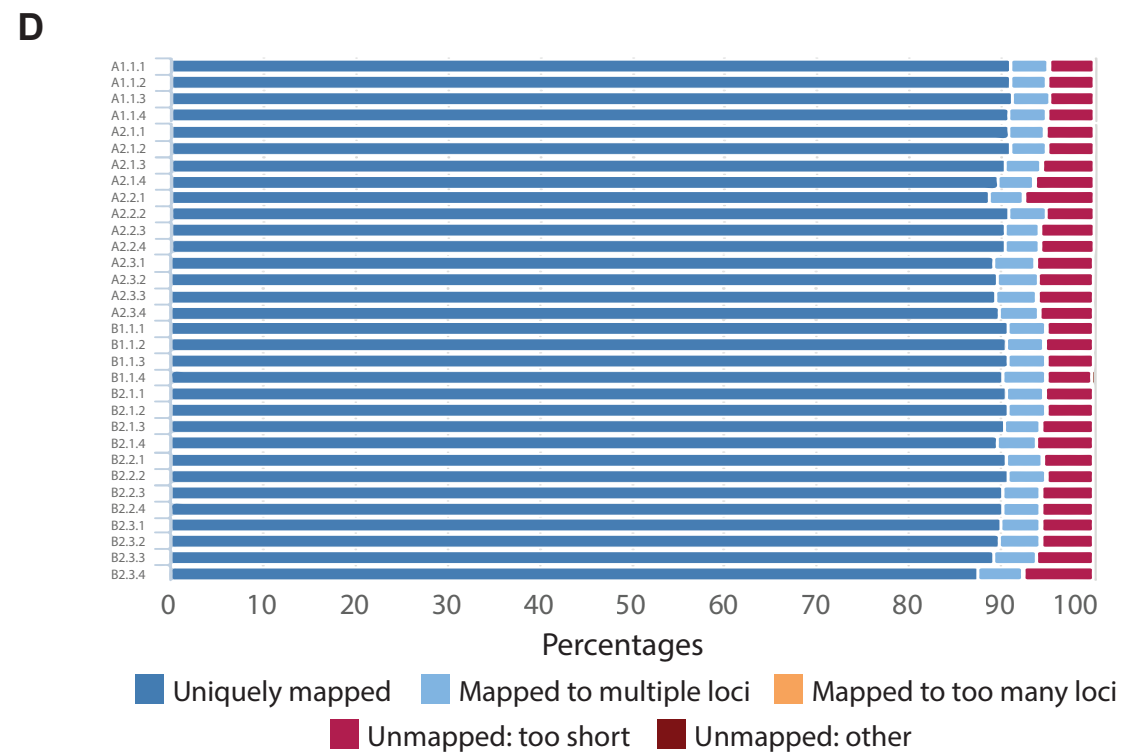
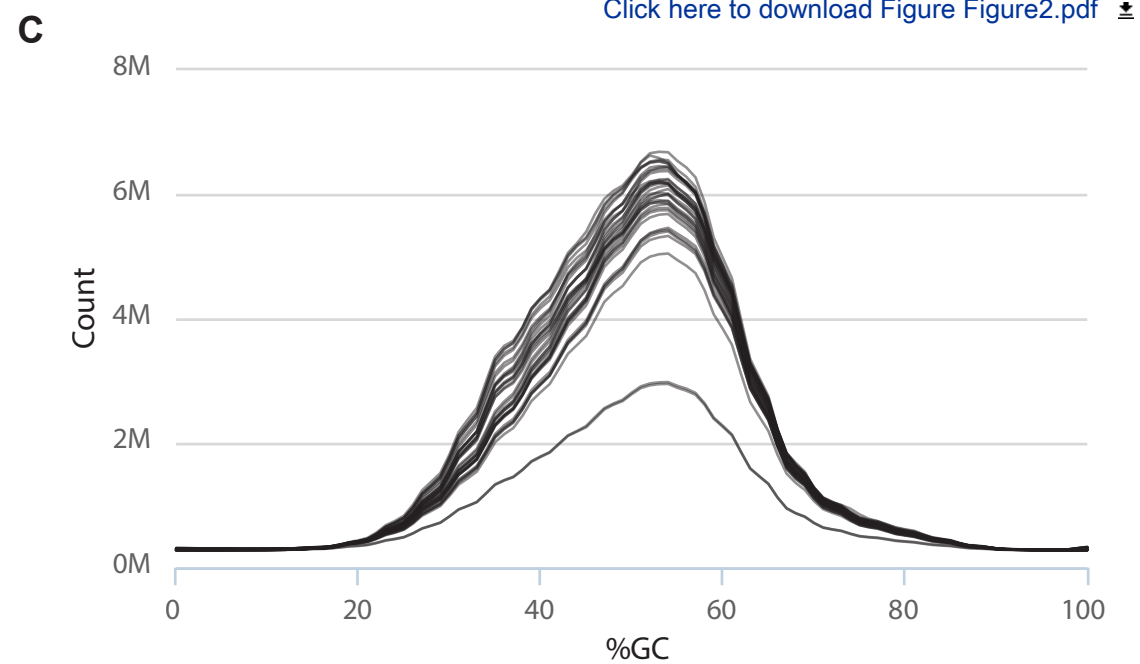
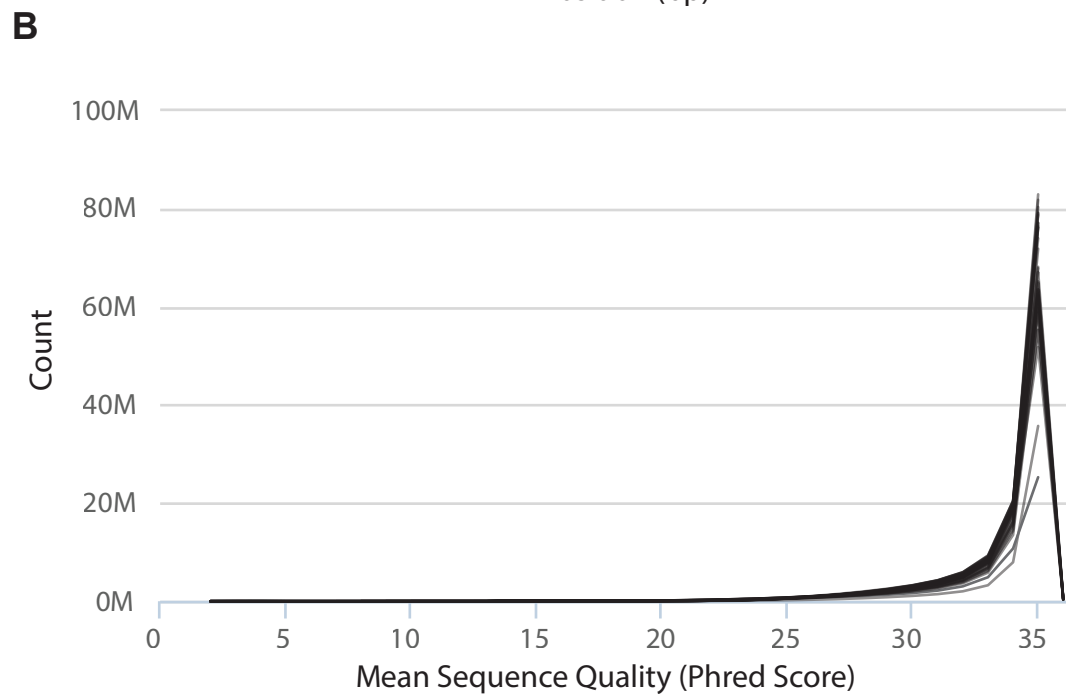
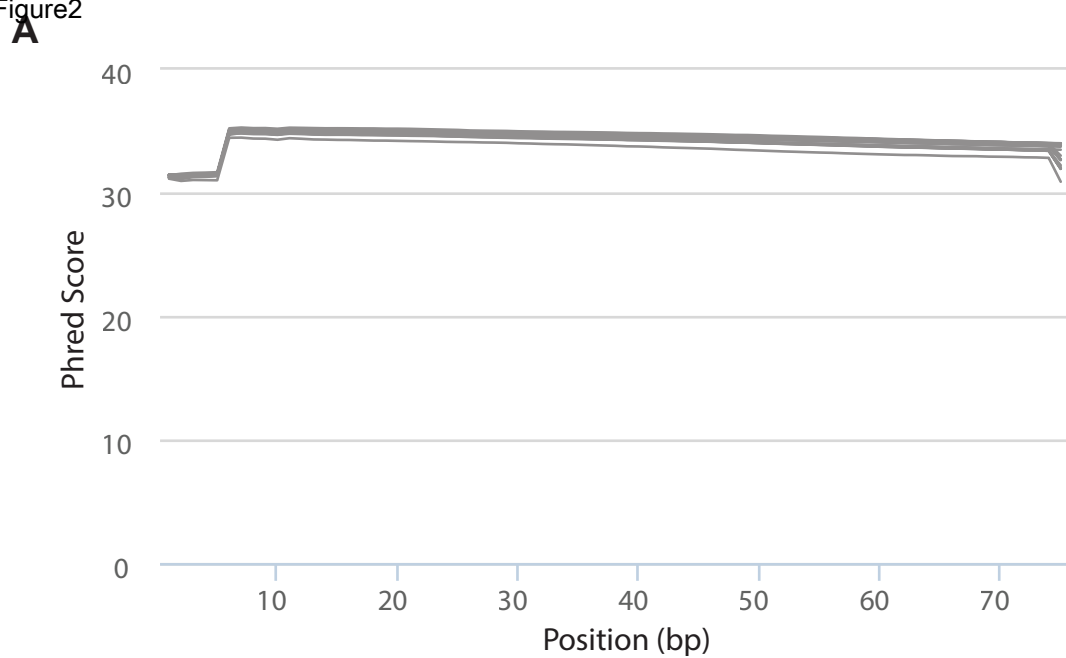


Figure3

[Click here to download Figure Figure3.pdf](#)

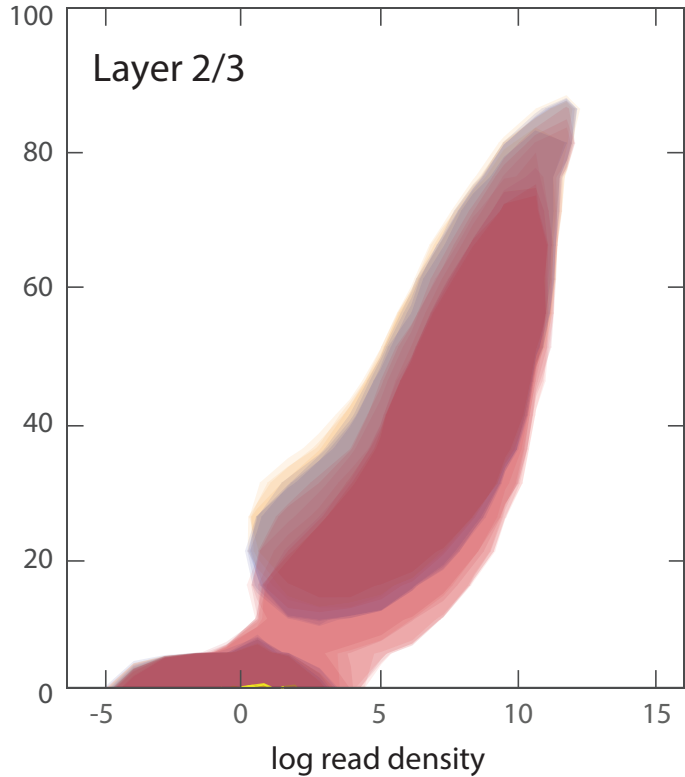
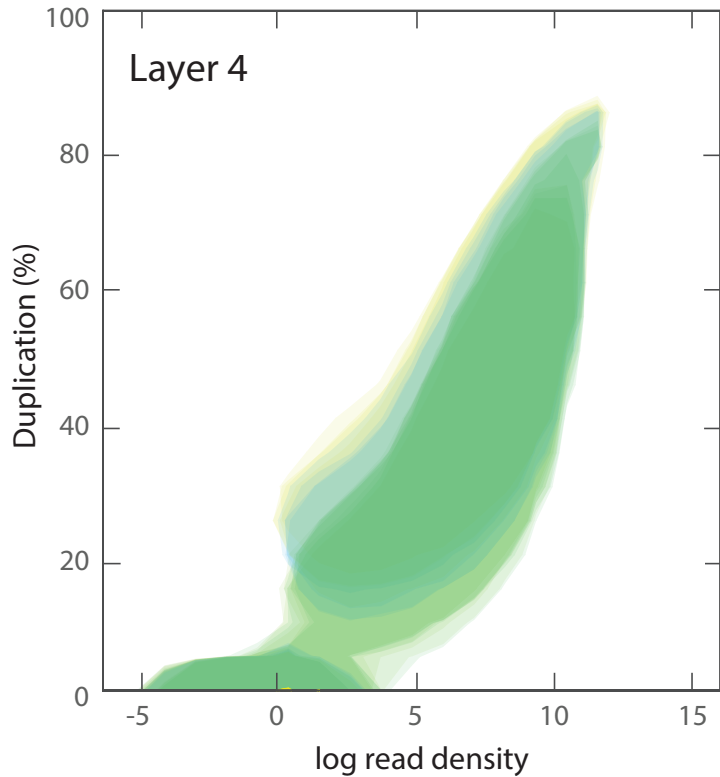
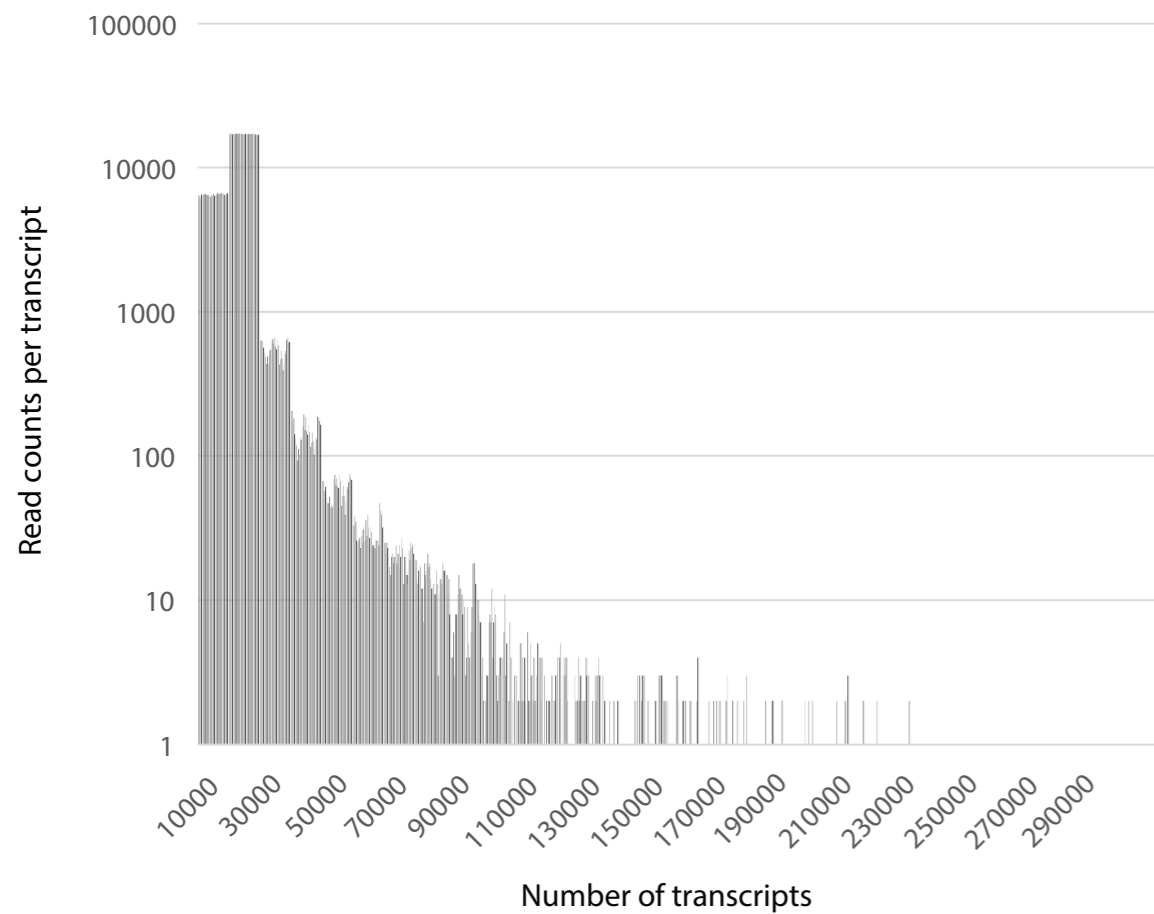
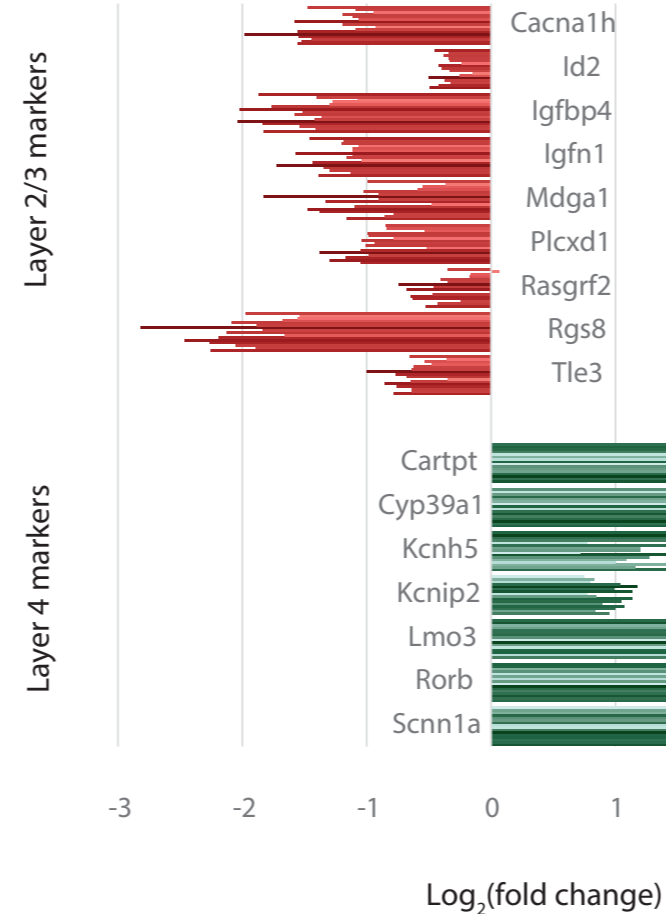


Figure4

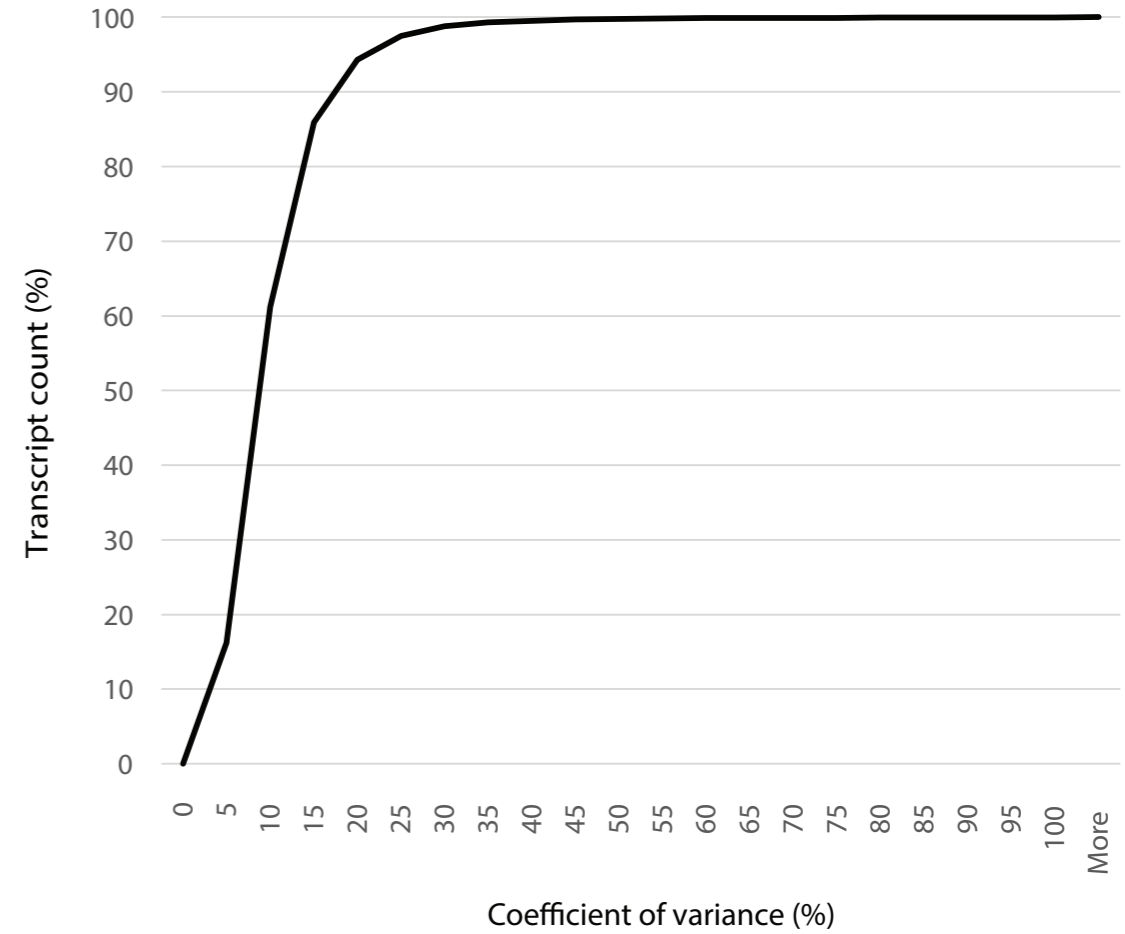
A



B



C







[Click here to access/download](#)

Supplementary Material

[Supplementary_Table1_EdgeRcommands.txt](#)

